JOURNAL OF Materials CHEMISTRY

A symmetric chiral liquid-crystalline twin exhibiting stable ferrielectric and antiferroelectric phases and a chirality-induced isotropic–isotropic liquid transition†

Isa Nishiyama,*[a] Jun Yamamoto,[a] John W. Goodby[b] and Hiroshi Yokoyama[a]

[a] *Yokoyama Nano-structured Liquid Crystal Project, JST, TRC 5-9-9 Tokodai, Tsukuba, Japan 300-2635*
[b] *Department of Chemistry, The University of Hull, Cottingham Road, Hull, UK HU6 7RX*

Received 15th June 2001, Accepted 6th August 2001
First published as an Advance Article on the web 2nd October 2001

In this article we report the first example of a pair of symmetrically substituted chiral twin enantiomers that exhibit stable wide temperature range ferrielectric and antiferroelectric phases, and which have large tilt angles of over 45°. In addition, both of the enantiomers exhibited an isotropic–isotropic liquid transition just above the transition to the liquid crystalline state.

1. Introduction

The discovery, in 1976, of ferroelectricity in smectic liquid-crystalline phases was particularly exciting because of its immediate applications to fast-response displays and light modulators. The later appearance of antiferroelectricity and ferrielectricity has made fundamental studies of chiral smectic liquid crystals even more fascinating. This is because these phases are thought to be generated through the delicate balance and competition of the intermolecular forces that determine the process of self-organization, and through the frustration created between the development of ferroelectric or antiferroelectric ordering that are respectively related to *synclinic* or *anticlinic* ordering of the molecules.

Thus far only a few systematic investigations have been reported which concern materials that were rationally designed to generate ferrielectric ordering.[1,2] Unlike *synclinic* or *anticlinic* phases, which can exist for achiral or chiral forms, the ferrielectric phase is essentially dependent on the presence of molecular chirality,[3] and indeed to our knowledge there are **no** examples of ferrielectric-like structures being exhibited by achiral materials. Thus, ferrielectric phases are part of the family of phases that have chirality-induced superstructures.

Two possibilities have been postulated for the origin of ferrielectric phases; one based on a distorted Ising model[4] and the other on a helical superstructure known as the clock model.[5] The ferrielectric phase has recently been confirmed to be highly biaxial and hence the structure has been considered to be modelled by a distorted structure,[6] which is also consistent with the other experimental results supporting a planar antiferroelectric structure.[7] Although a novel chiral structure that stabilizes the antiferroelectric phase has been reported,[8] examples of chiral materials that produce stable ferrielectric phases are limited. Consequently, a systematic exploration of new chiral materials is one of the more significant approaches towards the identification of design criteria for the synthesis of materials that exhibit stable ferrielectric phases. A particularly promising approach in this respect is the exploration of materials that have molecular twin architectures, which in some cases have been found to be useful in controlling chirality-dependent properties in terms of ferrielectric and antiferroelectric behaviour.[9] In terms of the design of twin systems it has been reported that homologous series of chiral twin compounds possessing two identical chiral moieties in the "inner" region of the molecular structure do not exhibit the ferrielectric phase, but instead exhibit the ferro- and antiferro-electric phases.[10] This result suggests that the location of the chiral moiety in the overall molecular structure plays an important role in the stabilisation of the ferrielectric phase. Alternatively, the introduction of chiral moieties at both ends of the central aromatic core of a molecular twin will allow for the chiral groups to interact with each other at the interfaces between the planes of the smectic layers. In this case, stronger chiral interactions between the neighbouring smectic layers will be obtained, and thus the chirality-induced superstructure of the ferrielectric ordering might be expected to become stabilized.

Thus here we report on the synthesis and liquid-crystalline properties of the optically active enantiomers of α,ω-bis(4-{[4′-(1-methylheptyloxycarbonyl)biphenyl-4-yl]oxycarbonyl}-phenoxy)hexane (**BMHBOP-6**)(Fig. 1), which is a liquid crystalline twin system with chiral moieties located towards the peripheral ends of the molecular structure. Through microscopic observation of the textures, differential scanning calorimetry (DSC), electro-optical studies, and powder X-ray diffraction measurements, **BMHBOP-6** was found to show stable ferrielectric and antiferroelectric phases (*ca.* 20 °C, respectively). Interestingly, the ferrielectric phase of the analogous monomeric homologous series, the 1-methylheptyl 4′-(4″-*n*-alkyloxybenzoyloxy)biphenyl-4-carboxylates, has been reported to be unstable for lower homologues, for example the octyl member shows no ferrielectric phase.[11] Thus, this is the first example that clearly demonstrates the significant efficacy of connecting two identical mesogenic groups in stabilising ferrielectric ordering. Furthermore, the absence of head–tail discrimination for this compound presents the first unequivocal evidence that the asymmetrical head–tail structure is not essential in generating the ferrielectric state.

2. Experimental

General preparative procedures

Both enantiomeric forms of the chiral twin **BMHBOP-6** were obtained by the esterification between optically active (*S*)- or (*R*)-1-methylheptyl 4-hydroxybiphenyl-4′-carboxylate and

---

†Basis of a presentation given at Materials Discussion No. 4, 11–14 September 2001, Grasmere, UK.

DOI: 10.1039/b105268n

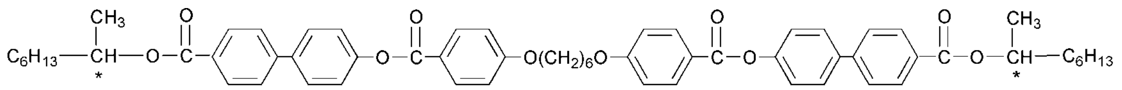

BMHBOP-6

Fig. 1 Molecular structure of **BMHBOP-6**.

α,ω-bis(4-carboxyphenoxy)hexane in the presence of 1,3-dicyclohexylcarbodiimide (DCC) and *N,N*-dimethylaminopyridine (DMAP). α,ω-Bis(4-carboxyphenoxy)hexane and the (*R*) and (*S*) optically active 1-methylheptyl 4-hydroxybiphenyl-4′-carboxylates were prepared according to standard procedures. In the synthesis the chiral alcohols, (*S*)-octan-2-ol (Azmax. Co. Ltd., 99% ee) and (*R*)-octan-2-ol (Azmax. Co. Ltd., 99% ee), were used without further purification.

Characterisation of materials

The purities of all of the final compounds were also checked by reverse-phase (ZORBAX, Eclipse XDB-C8) and normal-phase (CLC-SIL(M), Shimadzu) high-performance liquid chromatography. The structures of the materials were elucidated by a variety of spectral methods. Infrared (IR) spectroscopy was carried out using a Shimadzu FTIR-8100A infrared spectrophotometer, proton nuclear magnetic resonance (^{1}H NMR) spectrometry was carried out using a Bruker DRX500 (^{1}H NMR, 500 MHz) nuclear magnetic resonance spectrometer, and mass (MS) spectrometry was carried out using a JEOL, JMS-700 by using the FD/MS method. The analyses of the structures of the products and intermediates by spectroscopic methods were found to be consistent with the predicted structures.

X-Ray diffraction measurement

The X-ray scattering experiments were performed by real-time X-ray diffraction (Bruker AXS D8 Discover). The monochromatic X-ray beam (CuKα line) was generated by 1.6 kW X-ray tube and Göbel mirror optics. The 2D position sensitive detector had 1024 × 1024 pixels in a 5 cm × 5 cm beryllium window. A sample was fixed to a detector at a distance of 10 cm, so that the scattering angle dependence could be analyzed from 1.2 to 25° with 0.05° resolution (from 8 nm to 0.36 nm in real-space). A sample was introduced in a thin glass capillary (diameter 1.0 mm), which was placed in a custom-made temperature stabilized holder (stability to ±0.1 °C).

Preparation of (*S,S*)-α,ω-bis(4-{[4′-(1-methylheptyloxycarbonyl)biphenyl-4-yl]oxycarbonyl}phenoxy)hexane (*S,S*)-BMHBOP-6. (*S*)-1-Methylheptyl 4-hydroxybiphenyl-4′-carboxylate (1.30 g, 4.0 mmol), α,ω-bis(4-carboxyphenoxy)hexane (0.71 g, 2.0 mmol), and DMAP (0.05 g, 0.4 mmol) were added to dry dichloromethane (10 ml). DCC (1.23 g, 6.0 mmol) was then added and the resulting mixture was stirred at room temperature for one day. Precipitated material was removed by filtration. After removal of the solvent by evaporation under reduced pressure, the product was purified by column chromatography over silica gel (70–230 mesh, Sigma-Aldrich Co.) using a mixture of dichloromethane–hexane (5 : 1) as the eluent, and the resulting product was crystallised from a mixture of ethanol–ethyl acetate (1 : 4), to give a colourless solid. Yield = 0.79 g, (41%). δ_H (500 MHz, $CDCl_3$, TMS): 8.17 (m, 4H), 8.11 (m, 4H), 7.65 (m, 8H), 7.31 (m, 4H), 6.98 (m, 4H), 5.18 (m, 2H, $-C^*\mathbf{H}(CH_3)-$), 4.09 (t, 4H, $-C\mathbf{H}_2O-$), 1.89 (m, 4H, $-C\mathbf{H}_2CH_2O-$), 1.75–1.29 (m, 30H), 0.88 (t, 6H, $-C\mathbf{H}_3$). ν/cm^{-1} (KBr): 2940, 2850 (C–H str.), 1742, 1713 (C=O str.), 1607 (C–C str.), 845 (1,4-disub. C–H out of plane def.). *m*/*z*: 974 (M^+), 649, 487, 325. HPLC purity: normal phase Si column: 99.8%, reverse phase C8 column: 99.1%.

Preparation of (*R,R*)-α,ω-bis(4-{[4′-(1-methylheptyloxycarbonyl)biphenyl-4-yl]oxycarbonyl}phenoxy)hexane (*R,R*)-BMHBOP-6. This homologue was prepared from (*R*)-1-methylheptyl 4-hydroxybiphenyl-4′-carboxylate (1.30 g, 4.0 mmol) and α,ω-bis(4-carboxyphenoxy)hexane (0.77 g, 2.0 mmol), using the procedure described for (*S,S*)-**BMHBOP-6**, giving the product as a colourless solid. Yield = 0.84 g, (43%). δ_H (500 MHz, $CDCl_3$, TMS): 8.17 (m, 4H), 8.11 (m, 4H), 7.65 (m, 8H), 7.31 (m, 4H), 6.98 (m, 4H), 5.18 (m, 2H, $-C^*\mathbf{H}(CH_3)-$), 4.09 (t, 4H, $-C\mathbf{H}_2O-$), 1.89 (m, 4H, $-C\mathbf{H}_2CH_2O-$), 1.75–1.29 (m, 30H), 0.88 (t, 6H, $-C\mathbf{H}_3$). ν/cm^{-1} (KBr): 2940, 2850 (C–H str.), 1742, 1713 (C=O str.), 1607 (C–C str.), 845 (1,4-disub. C–H out of plane def.). HPLC purity: normal phase Si column: 99.9%, reverse phase C8 column: 99.9%.

3. Results and discussion

The phase transition temperatures for (*S,S*)-**BMHBOP-6** were found to be as follows: crystal 135.7 antiferroelectric SmC* 159.7 ferrielectric SmC* 178.7 ferroelectric SmC* 179.3 °C isotropic liquid. The results obtained for (*R,R*)-**BMHBOP-6** were found to be almost identical to those of its enantiomer, thereby demonstrating that change in molecular handedness has little or no effect on the liquid crystal properties.

Thermal polarised transmitted light microscopy was used to investigate the liquid-crystalline properties of the enantiomers. Both homogeneous (planar) and psuedo-homeotropic preparations were examined in order to give comparative defect textures. For the pseudo-homeotropic preparation of microscope specimens of (*S,S*)-**BMHBOP-6**, apparent textural changes were observed at the phase transitions to and from the smectic phases. The ferroelectric smectic C* phase showed a blue iridescent texture indicating that the helical structure of the phase had a pitch of approximately 0.2–0.4 μm. Conversely the ferrielectric and antiferroelectric phases were found to be non-iridescent, which in itself is interesting because the parent monomeric systems are strongly iridescent in both phases. However, at the transition between antiferroelectric and ferrielectric phases, characteristic textural changes, with constant defect motion similar to that reported for the analogous monomeric materials,[11] were observed. Remarkably, however, the racemic modification of **BMHBOP-6** exhibits a nematic phase at temperatures above the smectic C* to isotropic liquid phase transition. Thus, the nematic phase is stabilised for the racemic form.

Fig. 2 shows the differential scanning calorimetry (DSC) thermograms for (*S,S*)-**BMHBOP-6**. The (*S,S*)-isomer exhibits a sharp peak corresponding to the antiferroelectric–ferrielectric transition with a transition enthalpy of 0.44 kJ mol^{-1}, indicating that the transition is first order in nature. Just above the

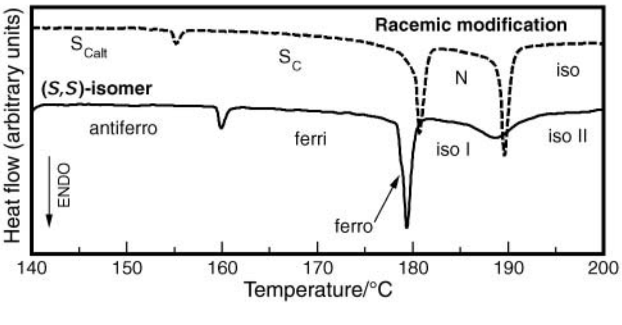

Fig. 2 Differential scanning thermograms obtained on heating for the (*S,S*)-enantiomer (solid lines) and the racemic modification (dotted lines), the scan rate was +5 °C min^{-1}.

clearing point, in a similar way to the situation found for the Twist Grain Boundary to liquid transition, there is a broad diffuse peak occurring in the isotropic liquid. The racemic modification on the other hand shows a sharp peak occurring at nearly the same temperature as the broad diffuse peak in the liquid phase for the enantiomers. The sharp peak this time, however, corresponds to a nematic to liquid transition. This result suggests that the effect of molecular chirality in twin systems considerably depresses the stability of the nematic phase.

The ferroelectric, ferrielectric and antiferroelectric properties were studied by the measurement of the apparent switching angle as a function of the applied electric field, in a cell with a 3 μm spacing that had been polyimide-coated and parallel-buffed. Since **BMHBOP-6** exhibits no smectic A* phase, large tilt angles of over 45° were observed as expected (see Fig. 3). In the ferroelectric phase, good bistability of the switched states was observed. In the ferrielectric phase, when the field is increased, the apparent tilt angle increases, changes its sense and reaches a saturated value corresponding to the electrically induced ferroelectric state *via* a metastable plateau corresponding to ferrielectric ordering. Switching in the antiferroelectric phase showed characteristic threshold behaviour with rather a large pre-transitional effect. A large saturated value of the tilt angle of 52° was obtained, and as a result this compound could be utilized as a component for increasing the tilt angle in eutectic mixtures of antiferroelectric materials. This is a particularly useful property to have for the development of materials to be used in devices based on a recently reported novel switching mode[12] that requires antiferroelectric materials with tilt angles of 45°.

X-Ray diffraction measurements show that diffuse scattering in the wide angle region was observed for all of the smectic phases of optically active **BMHBOP-6**, indicating that there is no long range positional order within the layers. This result is consistent with the fact that the ferro-, ferri- and antiferroelectric phases are the subphases of the smectic C phase. In the small angle region, a sharp peak corresponding to the smectic layer spacing was observed. The smectic layer spacing (d) and the apparent tilt angle (θ) obtained in the ferrielectric phase (13.7 °C below the ferrielectric to ferroelectric transition) are 4.2 nm and 45.5°, respectively, The $d/\cos\theta$ value of 6.0 nm was found to be comparable to the calculated molecular length of **BMHBOP-6** which was 5.6 nm. As **BMHBOP-6** itself does not exhibit the smectic A* phase the calculated value of 5.6 nm was determined from the layer spacing in the smectic A* phase, *i.e.*, 3.75 nm, measured for one of the analogous parent monomeric compounds, 1-methylheptyl 4′-(4″-*n*-decyloxybenzoyloxy)biphenyl-4-carboxylate (referred as **10B1M7**), and under the assumption that the average carbon–carbon distance is 0.14 nm. The difference between the calculated and measured molecular length may be attributed to the difference between the apparent optical tilt (θ) used for the calculation and the real steric molecular tilt.[13,14] Nevertheless, this result strongly suggests that the twin molecules form a monolayer structure but not an intercalated structure. If this is the case, then the two mesogenic groups of each twin molecule form a "pseudo" bilayer structure which allows the chiral moieties in proximity to the interfaces of the smectic layers, and therefore the chiral interactions between layers are expected to be relatively strong in comparison to monomeric systems.

Let us now consider the isotopric–isotropic liquid transition observed for optically active **BMHBOP-6**. The two isotropic phases show completely dark textures under examination using polarized light microscopy, however, as noted earlier, a bizarre diffuse peak above the smectic–isotropic liquid transition was observed in DSC thermograms, as shown in Fig. 2. XRD measurements show that the isotropic phases have no long range order so that these phases are not cubic or plastic crystal phases. The racemic modification (1 : 1 mixture of the optical isomers) shows no diffuse peak in the DSC thermogram, but shows a sharp peak corresponding to a nematic to isotropic liquid transition (Fig. 2, dotted line) even though the enantiomers themselves do not exhibit cholesteric phases. The nematic phase of the racemic modification was confirmed by the appearance of a planar *Schlieren* texture or a homeotropic dark texture observed under polarized light microscopy. So far, the appearance of the broad diffuse DSC peak in the isotropic region has been reported for some compounds showing a twist grain boundary (TGB) phase[15] or a cubic phase,[16] however, this behaviour has not been reported for the monomeric analogues[11] of **BMHBOP-6**. Thus, the connection of the two mesogenic parts may enhance the molecular assemblies responsible for the emergence of the isotropic–isotropic liquid transition.

It should be noted, finally, that the ferro-, ferri- and antiferro-electric phases have been found not to be miscible with those of the analogous monomeric compound, **10B1M7**. In the phase diagram, the continuity of the ferro-, ferri- and antiferro-electric phases of **BMHBOP-6** and **10B1M7** is interrupted by the injection of a smectic A* phase. Moreover, the characteristic filament texture,[17] which was observed for some of the binary mixtures, indicates that a TGB phase as well as a smectic A* phase was induced into the phase diagram.

In conclusion, we have demonstrated the first example of a symmetric chiral twin material showing: (i) a stable ferrielectric phase as well as the antiferroelectric phase, (ii) large tilt angles of over 45 degrees, and (iii) an isotropic–isotropic liquid transition.

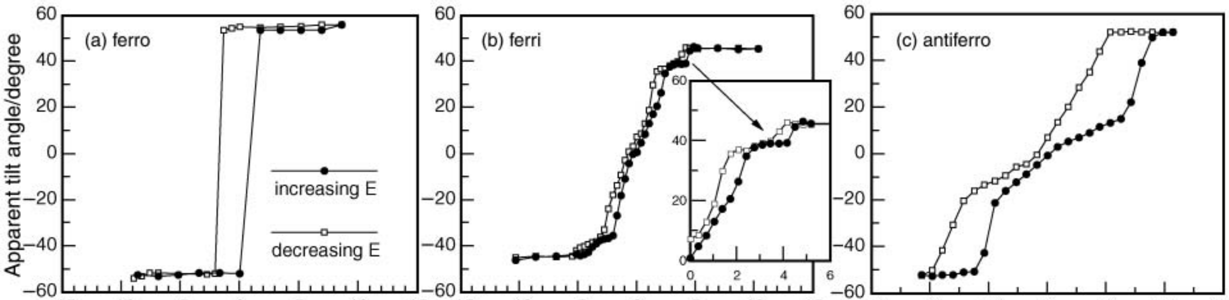

Fig. 3 The electric field dependence of the apparent tilt angle: (a) ferroelectric phase (0.7 °C below the clearing temperature), (b) ferrielectric phase (11.3 °C below the ferrielectric–ferroelectric transition), and (c) antiferroelectric phase (34.1 °C below the antiferroelectric–ferrielectric transition), solid circles indicate the tilt angles measured upon increasing the applied electric field, whereas open squares upon decreasing the electric field.

Acknowledgements

The authors thank Dr E. Nishikawa for X-ray diffraction measurements, and also thank Dr R.A. Lewis of the University of Hull for supplying a monomeric compound.

References

1 T. Matsumoto, A. Fukuda, M. Johno, Y. Motoyama, T. Yui, S. S. Seong and M. Yamashita, *J. Mater. Chem.*, 1999, **9**, 2051.

2 V. Faye, J. C. Rouillon, C. Destrade and H. T. Nguyen, *Liq. Cryst.*, 1999, **26**, 567.

3 H. Takezoe, J. Lee, A. D. L. Chandani, E. Grecka, Y. Ouchi, A. Fukuda, K. Terashima and K. Furukawa, *Ferroelectrics*, 1991, **114**, 187.

4 A. Fukuda, Y. Takanishi, T. Isozaki, K. Ishikawa and H. Takezoe, *J. Mater. Chem.*, 1994, **4**, 997, and references therein.

5 P. Mach, R. Pindak, A.-M. Levelut, P. Barois, H. T. Nguyen, H. Baltes, M. Hird, K. J. Toyne, A. J. Seed, J. W. Goodby, C. C. Huang and L. Furenlid, *Phys. Rev. E*, 1999, **60**, 6793; L. S. Matkin, H. F. Gleeson, P. Mach, C. C. Huang, R. Pindak, G. Sraijer, G. Pollmann, J. W. Goodby, M. Hird and A. J. Seed, *Appl. Phys. Lett.*, 2000, **76**, 1863.

6 P. M. Johnson, D. A. Olson, S. Pankratz, T. Nguyen, J. W. Goodby, M. Hird and C. C. Huang, *Phys. Rev. Lett.*, 2000, **84**, 4870.

7 M. A. Osipov and A. Fukuda, *Phys. Rev. E*, 2000, **62**, 3724.

8 Y. Aoki and H. Nohira, *Ferroelectrics*, 1996, **178**, 213.

9 I. Nishiyama and A. Yoshizawa, *Ferroelectrics*, 1996, **179**, 103.

10 Y. Suzuki, T. Isozaki, T. Kusumoto and T. Hiyama, *Chem. Lett.*, 1995, 719; Y. Suzuki, T. Isozaki, S. Hashimoto, T. Kusumoto, T. Hiyama, Y. Takanishi, H. Takezoe and A. Fukuda, *J. Mater. Chem.*, 1996, **6**, 753.

11 J. W. Goodby, J. S. Patel and E. Chin, *J. Mater. Chem.*, 1992, **2**, 197.

12 K. D'have, P. Rudquis, S. T. Lagerwall, H. Pauwels, W. Drzewinski and R. Dabrowski, *Appl. Phys. Lett.*, 2000, **76**, 3528.

13 J. W. Goodby, E. Chin, T. M. Leslie, J. M. Geary and J. S. Patel, *J. Am. Chem Soc.*, 1986, **108**, 4729.

14 J. T. Mills, H. F. Gleeson, J. W. Goodby, M. Hird, A. Seed and P. Styring, *J. Mater. Chem.*, 1998, **8**, 2385.

15 J. W. Goodby, A. Petrenko, M. Hird, R. A. Lewis, J. Meier and J. C. Jones, *Chem Commun.*, 2000, 1149.

16 S. Kutsumizu, T. Yamaguchi, R. Kato and S. Yano, *Liq. Cryst.*, 1999, **26**, 567.

17 J. W. Goodby, M. A. Waugh, S. M. Stein, E. Chin, R. Pindak and J. S. Patel, *J. Am. Chem Soc.*, 1989, **111**, 8119.